NeuroImage: Clinical 23 (2019) 101862

Contents lists available at ScienceDirect

NeuroImage: Clinical

journal homepage: www.elsevier.com/locate/ynicl

Cortical abnormalities in youth at clinical high-risk for psychosis: Findings from the NAPLS2 cohort

Yoonho Chung[a], Dana Allswede[a], Jean Addington[b], Carrie E. Bearden[c], Kristin Cadenhead[d], Barbara Cornblatt[e], Daniel H. Mathalon[f], Thomas McGlashan[g], Diana Perkins[h,i], Larry J. Seidman[j,k], Ming Tsuang[d], Elaine Walker[l], Scott W. Woods[g], Sarah McEwen[d], Theo G.M. van Erp[m], Tyrone D. Cannon[a,g,*], on behalf of the North American Prodrome Longitudinal Study (NAPLS) Consortium

[a] Department of Psychology, Yale University, 2 Hillhouse Ave., New Haven, CT 06520-8205, United States
[b] Hotchkiss Brain Institute, Department of Psychiatry, University of Calgary, 3280 Hospital Drive NW, Calgary, AB, T2N4Z6, Canada
[c] Semel Institute for Neuroscience and Human Behavior and Department of Psychology, UCLA, 760 Westwood Plaza, Los Angeles, CA, 90095, United States
[d] Department of Psychiatry, UCSD, 9500 Gilman Drive, La Jolla, CA 92093-0761, United States
[e] Department of Psychiatry, Zucker Hillside Hospital, 75-59 263rd St., Queens, NY 11004, United States
[f] Department of Psychiatry, UCSF, 401 Parnassus Avenue, San Francisco, CA 94143, United States
[g] Department of Psychiatry, Yale University, 300 George St., New Haven, CT 06511, United States
[h] Department of Psychiatry, University of North Carolina, 101 Manning Dr, Chapel Hill, NC 27514, United States
[i] Renaissance Computing Institute, University of North Carolina, Chapel Hill, United States
[j] Department of Psychiatry, Beth Israel Deaconess Medical Center and Harvard Medical School, 401 Park Drive, 2 East, Boston, MA 02215, United States
[k] Department of Psychiatry, Massachusetts General Hospital and Harvard Medical School, 401 Park Drive, 2 West, Boston, MA 02215, United States
[l] Department of Psychology, Emory University, 487 Psychology Building, 36 Eagle Row, Atlanta, GA 30322, United States
[m] Clinical Translational Neuroscience Laboratory, Department of Psychiatry and Human Behavior, UC Irvine, 5251 California Ave, Irvine, CA, 92617, United States

ARTICLE INFO

Keywords:
Magnetic resonance imaging
Clinical high risk
Psychosis
Brain development
Premorbid functioning
Schizophrenia

ABSTRACT

In a recent machine learning study classifying "brain age" based on cross-sectional neuroanatomical data, clinical high-risk (CHR) individuals were observed to show deviation from the normal neuromaturational pattern, which in turn was predictive of greater risk of conversion to psychosis and a pattern of stably poor functional outcome. These effects were unique to cases who were between 12 and 17 years of age when their prodromal and psychotic symptoms began, suggesting that neuroanatomical deviance observable at the point of ascertainment of a CHR syndrome marks risk for an early onset form of psychosis. In the present study, we sought to clarify the pattern of neuroanatomical deviance linked to this "early onset" form of psychosis and whether this deviance is associated with poorer premorbid functioning. T_1 MRI scans from 378 CHR individuals and 190 healthy controls (HC) from the North American Prodrome Longitudinal Study (NAPLS2) were analyzed. Widespread smaller cortical volume was observed among CHR individuals compared with HC at baseline evaluation, particularly among the younger group (i.e., those who were 12 to 17 years of age). Moreover, the younger CHR individuals who converted or presented worsened clinical symptoms at follow-up (within 2 years) exhibited smaller surface area in rostral anterior cingulate, lateral and medial prefrontal regions, and parahippocampal gyrus relative to the younger CHR individuals who remitted or presented a stable pattern of prodromal symptoms at follow-up. In turn, poorer premorbid functioning in childhood was associated with smaller surface area in medial orbitofrontal, lateral frontal, rostral anterior cingulate, precuneus, and temporal regions. Together with our prior report, these results are consistent with the view that neuroanatomical deviance manifesting in early adolescence marks vulnerability to a form of psychosis presenting with poor premorbid adjustment, an earlier age of onset (generally prior to the age of 18 years), and poor long-term outcome.

* Corresponding author at: Department of Psychology, 2 Hillhouse Avenue, New Haven, CT 06511, United States.
E-mail address: tyrone.cannon@yale.edu (T.D. Cannon).

https://doi.org/10.1016/j.nicl.2019.101862
Received 28 December 2018; Received in revised form 1 April 2019; Accepted 19 May 2019
Available online 23 May 2019

1. Introduction

Elucidation of biomarkers predictive of schizophrenia and other psychotic disorders is a high priority for the field. Neuroanatomical deviance, as assessed using quantitative metrics derived from magnetic resonance imaging (MRI) scans, has been suggested as potentially relevant to this goal. Several studies have observed a steeper rate of cortical thinning, particularly in heteromodal association regions, among clinical high-risk individuals (CHR) who convert to psychosis compared with those who do not convert and healthy controls (Borgwardt et al., 2008; Cannon et al., 2015; Chung et al., 2018; Pantelis, 2003; Sun et al., 2009, Takahashi et al., 2009). However, prior studies have obtained conflicting results as to whether individuals at CHR with poorer clinical and functional outcomes manifest measurable neuroanatomical deviance at the time of baseline evaluation (i.e. when help-seeking individuals were initially evaluated and met criteria for a psychosis-risk syndrome), as would be necessary if these measures are to have utility as *predictive* biomarkers (Borgwardt et al., 2007; Fusar-Poli et al., 2011; Mechelli et al., 2011; Pantelis et al., 2003; Takahashi et al., 2009; Velakoulis et al., 2006).

The wide age range of CHR samples (typically, 12–35 years) represents a major challenge for elucidation of neuroanatomical markers predictive of psychosis, given that deviance on such measures is only ascertainable with respect to age-appropriate norms, and there are marked developmental changes in brain structure across this age span (Brown et al., 2012; Gogtay et al., 2004; Tamnes et al., 2017). Further, given the heterogeneity in the timing of potentially relevant risk exposures and age at onset of prodromal symptoms and subsequent psychosis, the degree to which CHR cases manifest neuroanatomical deviance may well depend on their age at evaluation. Other factors that likely contribute to the inconsistent findings of prior MRI studies of CHR samples include the use of relatively small sample sizes and uneven application of statistical controls for multiple testing.

To overcome these limitations, we recently performed a machine-learning analysis of "brain age" using MRI measures in the North American Prodrome Longitudinal Study (NAPLS 2) sample (Chung et al., 2018). A neuroanatomical-based age prediction model was developed using a supervised machine learning technique with T1 MRI scans from the Pediatric Imaging, Neurocognition, and Genetics (PING) study and then applied to NAPLS2 scans for external validation and clinical application (Brown et al., 2012; Chung et al., 2018; Jernigan et al., 2016). The PING-derived model accurately predicted NAPLS healthy control subjects' chronological ages, providing evidence of independent, external validation. CHR individuals ascertained at younger ages (i.e., 12 to 17 years) were observed to show deviance from the normal neuromaturational pattern (i.e., a gap between "brain age" and chronological age), which in turn was associated with greater risk of conversion to psychosis and a pattern of stably poor functional outcome. In contrast, individuals who were 18 years of age or older showed age-normative neuroanatomical profiles at ascertainment (i.e., no gap between "brain age" and chronological age). A reevaluation of our prior findings showing a steeper rate of cortical thinning over time among CHR cases who converted to psychosis revealed that this effect was unique to the cases who were 18 years or older at ascertainment and did not apply to the younger cases (Cannon et al., 2015; Chung et al., 2018). This pattern is consistent with the view that neuroanatomical deviance manifesting in early adolescence marks vulnerability to a form of psychosis with an insidious onset and debilitating course of illness, while accelerated cortical thinning marks vulnerability to a more acute onset form of illness that does not manifest until late adolescence and early adulthood.

In the present study, we address two additional issues concerning the "early onset" form of psychosis. First, we aim to determine whether neuroanatomical deviance in early adolescence is associated with poorer premorbid functioning during childhood, as would be expected if this pattern is associated with a more insidious onset. Second, we aim to clarify whether the neuroanatomical deviance associated with onset of psychosis in early adolescence is distributed in brain regions previously linked to schizophrenia, including superior, medial, and dorsolateral prefrontal cortex, anterior cingulate, superior temporal cortex, and parahippocampal gyrus (Borgwardt et al., 2007; Fusar-Poli et al., 2011; Mechelli et al., 2011; Pantelis et al., 2003). Although the "brain age" approach can quantitatively assess deviations in brain maturation at the single subject level, a feature that makes it particularly useful for prediction purposes, the anatomical features selected by the algorithm are not necessarily indicative of risk for a particular disorder (Chung et al., 2018). By design, the fitted model parameters are data-driven, characterizing the regularized maturation pattern among brain structures that tracks with variations in chronological age among typically developing individuals. In other words, this "brain age" composite metric is not optimized for detecting schizophrenia risk per se and would presumably be sensitive to any condition in which cases deviate from the normal pattern of age-related neuroanatomical change during childhood/adolescence. Machine-learning algorithms trained to predict psychosis as an outcome could potentially yield a psychosis-specific pattern of neuroanatomical deviance (Koutsouleris et al., 2009). However, in the NAPLS2 study, such models were found to perform poorly compared with the "brain age" classifier, probably because the structural brain changes related to psychosis onset occur against the backdrop of the gradual gray matter decline that is part of normative adolescent brain development and because heterogeneity in the pathways leading to full psychosis works against the accuracy of machine learning algorithms trained on an outcome that treats all converters as exemplars of a unitary outcome class (Chung et al., 2018).

Here we report the results of group contrasts of the baseline MRI data according to 2-year clinical outcome in the same NAPLS2 sample that was used in the brain age prediction study. This analysis provides added value to the "brain age" prediction results in that it provides a more direct test of neuroanatomical changes associated with risk for psychosis and whether these effects are moderated by age at ascertainment and associated with poor premorbid adjustment. Based on the foregoing, we hypothesized that CHR individuals who are 17 years of age or younger would show smaller cortical volumes in dorsal lateral prefrontal cortex, medial prefrontal cortex, superior temporal gyrus, and parahippocampal areas. We also predicted that the younger CHR adolescents with persisting or worsening prodromal symptoms would show a greater degree of neuroanatomical deviance at baseline than those who are on the course of remission. We further hypothesized that the preexisting neuroanatomical deficits among younger CHR adolescents are associated with poorer premorbid functioning in childhood.

2. Material and methods

2.1. Participants

Participants were recruited through the NAPLS2 consortium, consisting of eight sites (UCLA, Emory, Beth Israel Deaconess Medical Center, Zucker Hillside Hospital, UNC, UCSD, Calgary, Yale) studying the psychosis prodrome in North America (Addington et al., 2012). The study protocols and informed consent forms for NAPLS2 were approved by the IRBs of all sites, and all procedures comply with the ethical standards of the relevant committees. The CHR cases met the Criteria of Prodromal Syndromes (COPS) based on the Structured Interview for Prodromal Syndromes (SIPS) for the presence of one or more of the three psychosis-risk syndromes: Brief Intermittent Psychotic Syndrome, Attenuated Positive Symptom Syndrome, and genetic Risk and Deterioration Syndrome (McGlashan et al., 2010).

Participants who meet criteria for attenuated psychotic symptom present onset or worsening of at attenuated positive symptoms in the past 12 months in at least one of the following five symptom domains: unusual thought content, suspicion/paranoia, grandiosity, perceptual anomalies, and disorganized communication. Participants also qualified

for a prodromal syndrome if they began displaying (in the past 3 months) brief intermittent positive psychotic symptoms below the threshold required for a DSM-IV axis I psychotic disorder diagnosis (First et al., 1995), or if they possessed a genetic risk for psychosis and displayed deterioration in functioning amounting to a 30% decline in their score on the Global Assessment of Functioning (GAF) scale in the past 12 months. Genetic risk was defined as a family history of psychosis in first-degree relatives or a diagnosis of schizotypal personality disorder. All North American Prodrome Longitudinal Study sites demonstrated good reliability employing the prodromal criteria (kappa range: 0.80–1.00 across sites) (Miller et al., 2002).

Subjects included in this report are those with MRI scans at baseline and with the latest follow-up SIPS assessment within 24 months or at the point of conversion to psychosis. Healthy control individuals were excluded if they met criteria for a psychotic disorder or Cluster A personality disorder, or showed prodromal signs, had a first-degree relative with a current or past psychotic disorder, or were on any psychotropic medication. As general criteria, individuals with past or current psychotic disorder, estimated IQ < 70, a central nervous system disorder, or substance dependence were excluded. Demographic characteristics of the three groups based on clinical outcome are shown in Table 1.

2.2. Defining outcome of CHR syndromes based on current clinical state

In CHR studies with longitudinal evaluation using the SIPS, the clinical outcome of interest has generally been based on classification of converters (CHR−C) versus non-converters (CHR-NC). However, given that only about 22% of the CHR individuals convert to psychosis within 1 year (Fusar-Poli et al., 2012), this approach results in a relatively small number of subjects in the CHR-C group (and an imbalance compared with the CHR-NC group for estimating means and variances), which significantly attenuates statistical power when performing group based statistics. In addition, while some of the non-converters show signs of remission at follow-up evaluation, some continue to exhibit sub-clinical symptoms of psychosis that persist or worsen over time (Addington et al., 2011). Therefore, in this study, we defined clinical outcome based on *Current Clinical State* criteria in the SIPS, which classifies clinical status by evaluating the course of symptoms in the month prior from the point of assessment (Woods et al., 2014). CHR individuals with partially ("symptomatic") or fully remitted prodromal symptoms at follow-up were grouped together and labeled as the "CHR-Stable/Remitted" group, whereas CHR individuals with persisting or progressing severity of prodromal symptoms or those who converted to psychosis were grouped together as the "CHR-Converted/Decline" group. This classification created a more balanced sample sizes and

Table 1
Demographic characteristics of participants.

	Age: 12–17				Age: 18–35			
	HC *N* = 52	CHR-Stable/Remitted N = 87	CHR-Decline N = 59	Statistical Test (2 tailed)/ *P* Value	HC *N* = 137	CHR-Stable/Remitted *N* = 131	CHR-Decline *N* = 100	Statistical Test (2 tailed)/ *P* Value
Age, mean(SD), y	14.99(1.43)	15.34(1.29)	15.26(1.15)	F = 1.23, *P* = .29	22.58(2.75)	22.33(2.53)	21.62(2.76)	F = 7.95, *P* < .001[e]
Male sex, No. (%)	37(69.8)	48(54.5)	29 (0.49)	$\chi2$ = 5.95, *P* = .050	61(44.5)	84(64.1)	66(66)	$\chi2$ = 14.73, *P* < .001
White /ethnicity, No. (%)	32(60.3)	47(53.4)	39(66.1)	$\chi2$ = 2.03, *P* = .362	75(54.7)	82(62.6)	61(61)	$\chi2$ = 1.88, *P* = .36
Hispanic or Latino /ethnicity, No. (%)	9	22	12	$\chi2$ = 0.23, *P* = .88	22(16.0)	16(12.2)	16(16)	$\chi2$ = 0.98, *P* = .61
Education level, mean (SD), y	8.35(1.45)	8.55(1.54)	8.62(1.19)	F = 16.02, *P* < .001[a]	14.78(2.24)	13.38(1.82)	13.24(1.83)	F = 23.26, *P* < .001[e]
Paternal education score, mean (SD)[g]	6.52(1.70)	5.69(1.57)	6.20(1.60)	F = 4.40, *P* = 0.013[b]	6.57(1.59)	6.60(1.65)	6.38(1.83)	F = 0.56, *P* = .57
Maternal education score, mean (SD)[g]	7.01(1.52)	6.31(1.62)	6.36(1.73)	F = 3.35, *P* = 0.037[b]	6.67(1.46)	6.45(1.52)	6.45(1.71)	F = 0.87, *P* = .41
Taking antipsychotics, No. (%) [h, i]	0(0)	17(33.3)	10(22.2)	$\chi2$ = 0.91, *P* = .33	0(0)	15(13.5)	20(22.9)	$\chi2$ = 3.00, *P* = .08
Scale of Prodromal Symptoms score, mean (SD)								
Positive	0.96(1.37)	11.09(3.99)	11.84(3.22)	F = 197.5 *P* < .001[d]	0.79(1.44)	12.0(3.86)	12.67(4.33)	F = 508.8 *P* < .001[d]
Negative	1.5(2.41)	11.86(6.14)	10.64(5.27)	F = 71.63 *P* < .001 [d]	1.25(1.96)	11.93(1.64)	12.58(6.59)	F = 189.6 *P* < .001[d]
Disorganization	0.67(1.18)	4.44(2.63)	5.41(3.48)	F = 49.59 *P* < .001 [d]	0.50(0.92)	5.01(3.16)	6.08(3.70)	F = 144.1 *P* < .001[f]
General	1.12(2.23)	8.61(4.24)	9.05(4.61)	F = 72.28 *P* < .001 [d]	1.33(2.11)	8.94(4.56)	9.12(3.85)	F = 192 *P* < 0.001[d]
PAS Total: Childhood	0.11(0.09)	0.26(0.18)	0.29(0.17)	F = 22.00 *P* < 0.001 [d]	0.12(0.11)	0.23(0.17)	0.22(0.16)	F = 21.95 *P* < 0.001[d]
GAF Score at Baseline	84.15(11.74)	50.62(11.57)	48.86(10.97)	F = 172.30 *P* < 0.001 [d]	84.84(9.41)	48.60(12.19)	47.29(10.01)	F = 515.2 *P* < 0.001[d]

Post hoc Tukey Test: [a]HC < CHR-Stable/Remitted, CHR-Decline, [b]CHR-Stable/Remitted < HC, CHR-Decline, [c]CHR-Stable/Remitted, CHR-Decline < HC, [d]HC < CHR-Stable/Remitted, CHR-Converted/Decline, [e]CHR-Stable/Remitted, CHR-Decline < HC, [f]HC < CHR-Stable/Remitted < CHR-Decline.

Abbreviations: CHR, clinically high-risk individuals; GAF, Global Assessment of Functioning; HC, healthy controls; NA, not applicable; PAS, premorbid adjustment scale.

g Parental education scored as follows: 1, no schooling; 2, some primary school; 3, completed primary school; 4, some high school; 5, completed high school; 6, some college, technical school, or undergraduate education; 7, completed college, technical school, or undergraduate education; 8, some graduate or professional school; and 9, completed graduate or professional school.

h Because this was a naturalistic study, individuals were treated in their respective communities according to prevailing standards and the judgment of the treating clinicians, who were often primary care physicians rather than psychiatrists.

i $\chi2$ Test performed within CHR group.

variability in each group (CHR-Stable/Remitted: $N = 219$, CHR-Converted/Decline: $N = 159$).

2.3. MRI data acquisition

Five sites (University of California, Los Angeles, Emory University, Harvard University, University of North Carolina, and Yale University) operated Siemens scanners and three sites operated GE scanners (Zucker Hillside Hospital, University of California, San Diego, University of Calgary). Magnetic field strength for all scanners were 3 Tesla. Siemens sites used a 12-channel head coil and the GE sites used an 8-channel head coil. Sequence parameters were optimized for each scanner manufacturer, software version and coil configuration according to the ADNI protocol (http://adni.loni.ucla.edu/research/protocols/mri-protocols/) (Mueller et al., 2005). At all sites, scans were acquired in the sagittal plane with a 1 mm × 1 mm in-plane resolution and 1.2 mm slice thickness. Siemens scanners used an MPRAGE sequence with a 256 (axial) x 240 (sagittal) x 176 (coronal) mm field of view, TR/TE/TI52300/2.91/900 ms and a 9 degree flip angle, while GE scanners used an IR-SPGR sequence (efgre3d_cs) with a 26 cm field of view, TR/TE/TI57.0/minimum full/ 400 ms and an 8 flip angle (Cannon et al., 2013).

2.4. Image processing

Automated surface based cortical reconstruction, cortical parcellation and subcortical segmentation were performed using the Freesurfer software suite version 5.3 (http:// surfer.nmr.mgh.harvard.edu/) (Dale et al., 1999; Fischl, 2004; Fischl and Dale, 2000; Fischl et al., 2002; Fischl et al., 1999). Regional parcels for gray matter volume, cortical thickness and surface area were extracted using a gyral and sulcal pattern based Desikan atlas with 34 parcels in each hemisphere (Desikan et al., 2006).

2.5. Adjusting for scanner-specific offsets

Although the scanners used in this study were all 3 Tesla systems with standardized pulse sequence parameters across all sites, scanner related noise that is specific to manufactures, models, coil configuration, field inhomogeneity and other idiosyncratic signatures that are unique to each scanner could still contribute noise to the anatomical measurements (Cannon et al., 2013; Dewey et al., 2010; Nugent et al., 2013; Schnack et al., 2010). Therefore, we tried to further improve between-site reliability by modeling scanner related variance in the regression of age among typically developing adolescents and young adults (i.e., NAPLS2 healthy controls) with a linear mixed effects model. Age, sex, and ICV were treated as fixed factors and scanner ID was treated as a random intercept for each neuroanatomical measure. After fitting the model, random intercept parameters fitted for each scanner were derived to adjust the differing intercepts of age regressions across scanners for both healthy controls and CHR cases. This approach capitalizes on an assumption that there is a true “fixed” slope of age in a typically developing population for a given neuroanatomical region; the assumption is widely supported by previous studies that have consistently shown that the shape of the non-linear age trajectories, between childhood and early adulthood, for a given structural brain measure are remarkably parallel across multiple independent datasets (Gogtay et al., 2004; Tamnes et al., 2017; Tamnes et al., 2010). This pattern was also observed in our dataset when age-trajectories were modeled separately by each scanner (see Fig. 1). For the purpose of estimating the variance of scanner as a random effect, the age trajectories were modeled only among healthy controls, as the age-related variance in the CHR group would be more variable due to the heterogeneity in the underlying disease process. Although it is well known that the shape of the developmental trajectories for neuroanatomical measures is best characterized as a non-linear process (Fjell et al., 2010), fitting a linear model is appropriate to prevent overfitting of the data, especially for sites with small sample size. MRI scanners that assessed less than ten control subjects were dropped from this analysis because scanner related variance could not be reliably modeled. For this reason, a total of 20 controls and 67 CHR cases (6 of whom were converters) were excluded from the analysis.

2.6. Human traveling subjects

MRI scanner reliability and the effectiveness of the statistical correction method implemented in this study to reduce scanner related variance were assessed using human traveling subjects data. Detailed information about the human traveling subjects, scanning equipment, and prior reliability study results are documented in previous publications (Cannon et al., 2013). Briefly, each of these sites recruited one healthy subject (4 males, 4 females) between the ages of 20 and 31 (mean = 26.9, SD = 4.3), who was scanned twice on successive days at every site for a total of 128 scans (8 subjects × 2 scans × 8 sites). Scanning was conducted from May 4 through August 9 of 2011. There were no equipment or software changes at any of these sites during this period.

2.7. Assessment of reliability across scanners

Using the human traveling subjects data, variance components analysis based on linear mixed-effects modeling was performed to calculate intra-class correlations (ICC) with restricted maximum likelihood (REML) estimates. Given that the three factors (subject, site, occasion) were fully crossed, the total variance of the dependent variable was decomposed into the variance due to subject, site, occasion, subject-by-site, subject-by-occasion, site-by-occasion, and subject-by-site-by occasion, with each factor treated as a random effect (Cannon et al., 2013; Friedman et al., 2007). The model is as followed, with σ^2 denoting the variance of a dependent measure X for subject = i, site = j, and visit = k. The residual variance is expected to represent a combination of three-way interaction and residual error, with e denoting unexplained variance due to error:

Two types of ICCs were computed: Between-site ICC (ICCBW) and within-site ICC (ICCWI). ICCBW is measured by the fraction of variance attributable to subject, reflecting reliability across sites and occasions. ICCWI is measured by the fraction of variance attributable to subject and site, reflecting reliability across scan occasions for the same subject at the same site. The specific formulae used were:

$$\sigma^2(X_{ijk}) = \sigma^2{}_i + \sigma^2{}_j + \sigma^2{}_k + \sigma^2{}_{ij} + \sigma^2{}_{ik} + \sigma^2{}_{kj} + \sigma^2 i_{jk,e}$$

$$ICC_{BW} = \sigma^2{}_{Subject}/\sigma^2{}_{Total}$$

$$ICC_{WI} = (\sigma^2{}_{Subject} + \sigma^2{}_{Site} + \sigma^2{}_{Subject\ by\ Site})/\sigma^2{}_{Total}$$

where σ^2 refers to variance due to the factor(s) denoted by subscript. This formulation of the within-site ICC produced results equivalent to the test-retest ICC averaged across sites. ICCs can range from 0.0 to 1.0, and results were interpreted according to the following recommendations: poor (below 0.40), fair (0.41–0.59), good (0.60–0.74), and excellent (above 0.75) (Cicchetti and Sparrow, 1981).

2.8. Premorbid adjustment scale

The premorbid adjustment scale (PAS) is one of the most commonly used interview-based retrospective rating scales in schizophrenia for assessing premorbid functioning (Cannon-Spoor et al., 1982; Van Mastrigt and Addington, 2002). This scale assesses sociability and social withdrawal, peer relationships, scholastic performance, adaptation to school, and the ability to form socio-sexual relationships across four different developmental periods of development: childhood (age 5–11), early adolescence (age 12–15), late adolescence (age 16–18), and

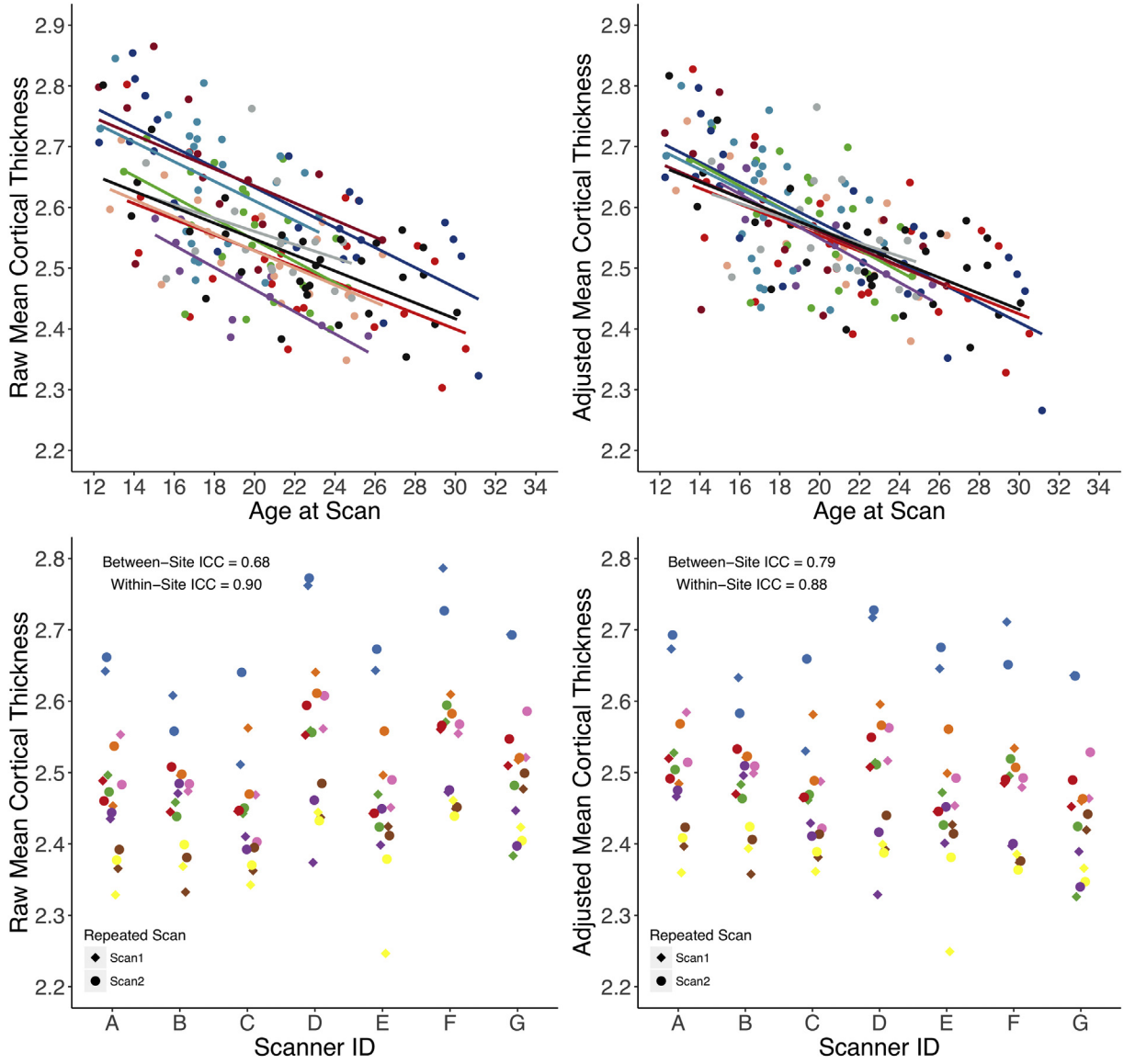

Fig. 1. In the upper panels, mean cortical thickness of NAPLS2 healthy controls is plotted as a function of age before (upper left) and after (upper right) adjusting for the scanner offsets. The solid lines represent least-square linear fits and the colors correspond to different scanners used. In the lower panels, mean cortical thickness of human traveler subjects are plotted across selected scanners. (Lower left) Mean cortical thickness before adjusting for scanner offsets. (Lower right) Mean cortical thickness after adjusting for the offsets. Colors and shape correspond to human phantom ID and scan time points, respectively.

adulthood (age 19 and above) (Cannon-Spoor et al., 1982). As premorbid functioning was defined as the period preceding the onset of the first attenuated psychotic symptom that contributed to the participant meeting COPS criteria, PAS ratings beyond the childhood period were not applicable for CHR individuals in early adolescence (age 12–17) (Lyngberg et al., 2015). Premorbid functioning was dichotomized into "poor" and "good" functioning group, by using a cutoff that is 1.5 SD above the mean in the healthy control group (0.38 of the total PAS score in childhood ranging from 0.0 to 1.0). Median PAS score in the CHR group (PAS = 0.22) was also tested as an alternative way to define the threshold.

2.9. Statistical analyses

Previous whole-brain analyses that contrasted individuals with attenuated symptoms of psychosis (e.g., CHR, ARMS, psychosis spectrum symptoms etc.) to healthy controls have mainly used the VBM method and treated age as a covariate of non-interest to control for normative neurodevelopmental effects. In order to compare our results with other independent studies, we adapted the previously used statistical models as closely as possible and applied them to the NAPLS2 data. Statistical whole-brain maps were generated and *P* values for comparisons between individuals at CHR and healthy controls were mapped at each vertex. Linear mixed models were fitted at each vertex across the surface, with cortical volume, area, and thickness as dependent variables, after partialing out the effects of age, sex, and ICV. Scanner offsets were estimated as random effects and adjusted using the linear mixed model as proposed above. Z Monte Carlo simulations, one of the features implemented for multiple comparison correction in FreeSurfer (Hagler, Saygin, & Sereno, 2006; Hayasaka, 2003), was applied with a cluster-forming threshold of $P < .05$ (two-sided). Uncorrected P values were displayed within the thresholded clusters at $P < .05$.

For all group level analyses based on clinical outcome, a generalized additive model (GAM) from the "mgcv" package in R Version 3.1.0. [http://www.r-project.org/] was used to better characterize non-linear trajectories of structural brain development. GAM fitting has shown to have some advantages over the use of polynomial models, as the shape of the function does not have to be pre-defined, and the placement of

the peaks of these polynomial fits could be erroneously variable depending on the age-range sampled for a study (Fjell et al., 2010). Nonparametric smoothing splines were fitted for the age term to allow greater flexibility without any restrictions on the shape of the curve. Degree of smoothness was defined using the thin plate regression spline and was regularized based on restricted maximum likelihood to guard against overfitting. Group status and other potential confounding variables such as sex, maternal education, ethnicity and ICV were also tested as conventional parametric linear terms. Significance of the age by group interaction term was tested with analysis of variance (ANOVA) in the *mgcv* package.

Neuroanatomical measures for all subjects were transformed into Z scores based on the means and standard deviations of the control group, after partialing out variance associated with age, sex, ICV, and scanner using the GAM fitting method as described above. Study participants were then partitioned into an early adolescent group (age range: 12–17) and a later adolescent/young adult group (age range: 18–35). As effect sizes are expected to be modest and statistical power is significantly reduced due to partitioning the sample based on age, a series of statistical tests was performed in a hierarchical manner. First, the global measures of cortical volume, cortical thickness, and surface area were tested. If significant association was detected at the global level, then parcels from the Desikan atlas of both hemispheres were utilized to examine regional specificity. False discovery rate (FDR) was set to 5% for testing 68 ROIs (34 ROIs per hemisphere) per cortical index (i.e. cortical thickness, surface area, cortical volume) to correct for multiple comparisons (Benjamini and Hochberg, 2000). We did not implement vertex-wise whole brain analysis for the partitioned sample by age, as this method requires substantial statistical power to survive the stringent correction for multiple comparisons that is imposed for testing all vertices. Subcortical and ventricular volume measures (31 structures) were also tested using the same approach (Fischl et al., 2002). This strategy was also implemented when performing tests in relation to antipsychotic medications and premorbid functioning.

For discerning regional neural correlates of clinical outcome within the CHR individuals, we performed a priori hypothesis testing to reduce the risk of being underpowered (false-negative). We predicted that CHR-Converted/Decline group would show cortical deficits in lateral and medial prefrontal, parahippocampal, anterior cingulate, and superior temporal regions relative to CHR-Stable/Remitted group, as these regions were most frequently implicated in predicting clinical outcomes among high-risk individuals (Borgwardt et al., 2007; Fusar-Poli et al., 2011; Mechelli et al., 2011; Pantelis et al., 2003).

3. Results

3.1. Adjusting scanner-specific variance using age-related developmental patterns

For nearly all of the neuroanatomical measures, ICC_{WI} values were in the excellent range (median = 0.92, 1st quantile = 0.85, 3rd quantile =0.96). Before correcting for scanner effects, ICC_{BW} values generally ranged from good to excellent for surface area, cortical volume, and subcortical volume measures, while ICC_{BW} values for cortical thickness measures generally ranged from fair to good. However, when cortical thickness measures were adjusted based on the random intercept age regression parameters fitted for scanner ID, the ICC_{BW} values generally improved towards good to excellent. As shown in the upper panels of Fig. 1, mean cortical thickness as a function of age among healthy controls is plotted for both before and after scanner correction parameters were applied. Ordinary least square age regression fits for mean cortical thickness converged and the ICC_{BW} improved from good (ICC_{BW} = 0.68) to excellent (ICC_{BW} = 0.79). Descriptive statistics and interpretations for the between-site ICCs are summarized in Table 2. The frequency distribution of ICC_{BW} values, for both raw and post-scanner adjustment values, are shown in Fig. 2. Raw and adjusted ICC_{WI} and ICC_{BW} values for all neuroanatomical ROIs evaluated are presented in the supplementary materials. Scanner-corrected neuroanatomical measures were used for all subsequent analyses.

3.2. Cortical gray matter deficits in individuals at clinical high-risk

Based on GAM analysis, CHR individuals exhibited significantly smaller total cortical volume ($t = -3.49$, $P < .001$), total surface area ($t = -2.56$, $P = .012$), and mean thickness ($t = -3.34$, $P < .001$) compared with healthy controls (CHR: $n = 428$, HC: $n = 205$). A significant interaction between age and CHR status was observed for cortical volume ($P = .009$) and surface area ($P = .039$), but the interaction term for cortical thickness did not reach significance ($P = .16$). Penalized regression splines were fitted to each cortical measure as a function of age and were visually inspected. As shown in Fig. 3, the 95% confidence intervals for GAM fitted splines did not overlap among individuals between approximately 12 and 17 years of age. Significantly smaller cortical indices were observed among the CHR adolescents who were under 18 years of age (volume: $t = -3.90$, $P = .005$; surface area: $t = -2.8$, $P = .018$; thickness: $t = -2.84$, $P = .016$; CHR = 197, HC = 68). There were no group differences among subjects who were 18 years of age or older (P values over 0.33).

In order to examine the spatial patterns of cortical deficits in CHR cases, vertex-wise whole brain analysis was conducted for each cortical measure. As shown in Fig. 4, CHR individuals exhibited widespread, significantly smaller areas of cortical volume, surface area, and cortical thickness relative to controls after correcting for multiple comparisons. In terms of surface area, CHR individuals showed significant reduction in multiple brain areas including dorsolateral prefrontal, medial prefrontal, parahippocampal, fusiform area, and temporal regions. Reduced cortical thickness was observed in lateral occipital, pre- and post-motor regions, parietal cortex, and temporal cortices. As cortical volume is a composite measure of thickness and area at each vertex, many of the clusters with diminished cortical volume substantially overlapped with significant clusters revealed in surface area and cortical thickness maps.

3.3. Neuroanatomical correlates of clinical outcome in CHR individuals

In the younger adolescent group, CHR individuals with a remitted or stable pattern of prodromal symptoms at follow-up (i.e. CHR-Stable/Remitted) showed significant reductions in cortical volume ($t = -3.02$, $P = .002$) and cortical thickness ($t = -2.39$, $P = .020$) at baseline compared with healthy controls (CHR-Stable/Remitted $n = 87$, healthy controls $n = 52$; see Fig. 5; for regional specificity, see Table 3). CHR cases who converted or had worsening symptoms (i.e., CHR-Converted/Decline) exhibited reduced cortical volume ($t = -4.04$, $P < .001$), surface area ($t = -3.56$, $P = .0004$, $n = 111$), and cortical thickness ($t = -2.30$, $P = .027$) compared with controls (CHR-Decline: $n = 59$, HC: n = 52; see Fig. 5; for regional specificity, see Table 4). There were no significant group differences on any of the neuroanatomical measures in the older group ($Ps > 0.48$). Group differences in the deep brain structure and ventricular volume measures were not observed across all age ranges ($Ps > 0.28$).

As we hypothesized from prior work, the CHR-Converted/Decline group showed smaller surface area in rostral anterior cingulate, lateral and medial prefrontal regions, and parahippocampal gyrus relative to the CHR-Stable/Remitted group, among younger adolescents only (CHR-Stable/Remitted: n = 87, CHR-Converted/Decline: n = 59; see Table 5 for the list of ROIs). However, there were no significant differences in area of superior temporal gyrus and in any of the regional cortical thickness measures. To supplement our results, we also performed identical set of analyses to our cohort that is grouped into CHR-C vs CHR-NC. The results are presented in the supplementary materials.

Table 2
Descriptive statistics of between-site ICC across neuroanatomical measures before and after adjusting for scanner offsets.

Type of neuroanatomical measure[a]	Between-site ICCs for all ROIs							
	Median		1st quantile		3rd quantile		Interpretation[b]	
	Raw	Adjusted	Raw	Adjusted	Raw	Adjusted	Raw	Adjusted
Cortical thickness	0.63	0.69	0.51	0.60	0.73	0.77	Fair ~ Good	Good ~ Excellent
Surface area	0.87	0.91	0.84	0.86	0.94	0.95	Excellent	Excellent
Cortical volume	0.87	0.90	0.78	0.80	0.92	0.93	Excellent	Excellent
Subcortical volume	0.84	0.86	0.71	0.74	0.92	0.94	Good ~ Excellent	Good ~ Excellent

[a] Cortical parcellations (34 ROIs per hemisphere) were defined using the Desikan atlas (Desikan et al., 2006). Selected deep brain structure volumes were derived by automatic subcortical segmentation pipeline using Freesurfer (Fischl et al., 2002).
[b] Interpretations were made based on the range between 1st and 3rd quantiles.

3.4. Poor premorbid functioning is linked to structural brain abnormalities in younger CHR adolescents

Finally, we tested whether neuroanatomical deficits observed in early adolescence were associated with poor premorbid functioning. As shown in Fig. 6, younger subjects (CHR and healthy control subjects combined; PAS good: n = 111, poor: n = 87) with relatively poor premorbid functioning showed smaller cortical volume ($t = 3.68$, $P < .001$) and surface area ($t = 2.88$, $P = 0.001$), but no difference was observed in cortical thickness ($t = 1.95$, $P = .062$) than the good premorbid functioning group; suggesting that the observed smaller cortical volume is mainly driven by a smaller surface area. When group

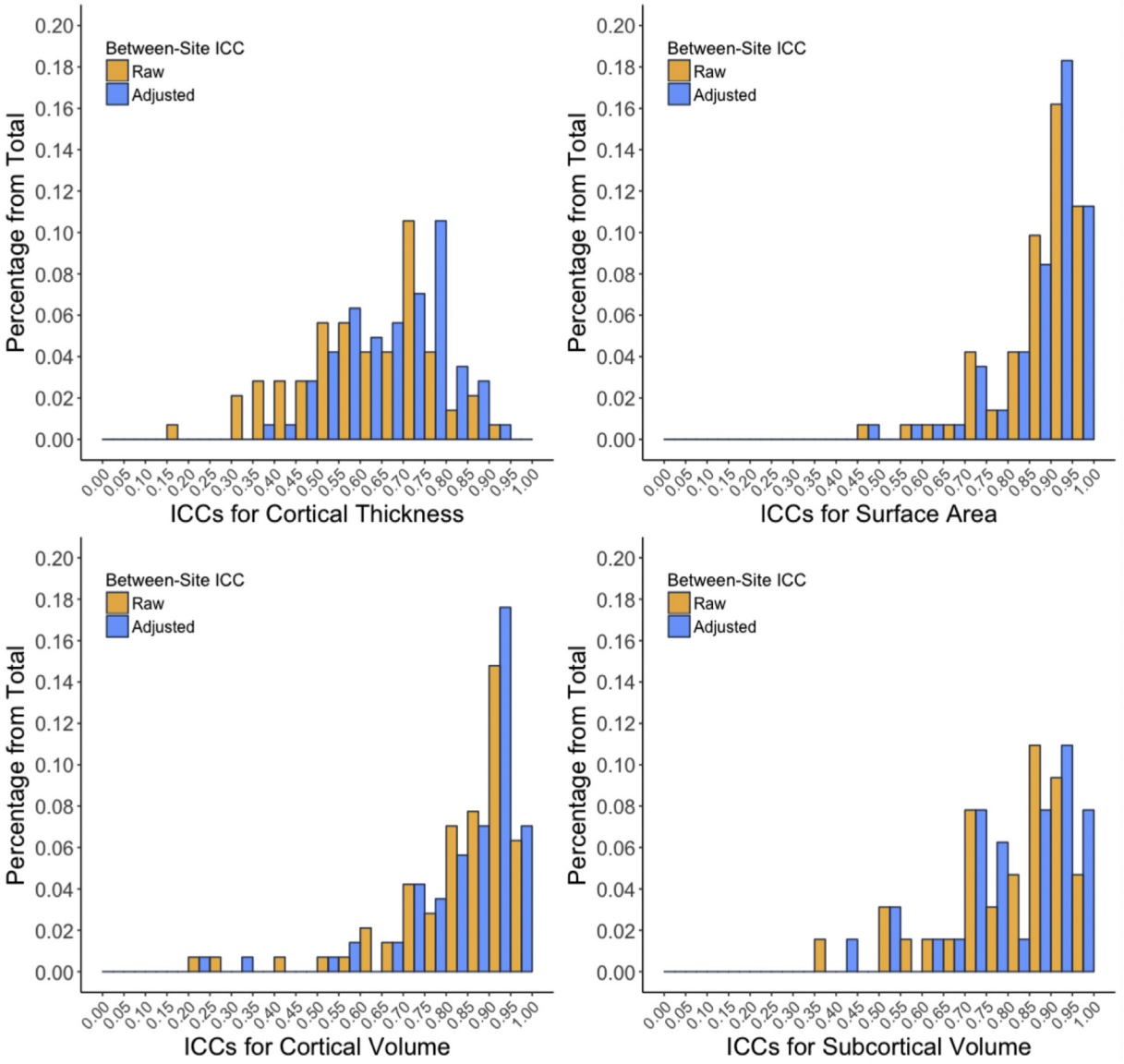

Fig. 2. Frequency distribution of between-site ICCs both before and after adjusting for the scanner offsets across all neuroanatomical Desikan based ROIs and subcortical segmentations.

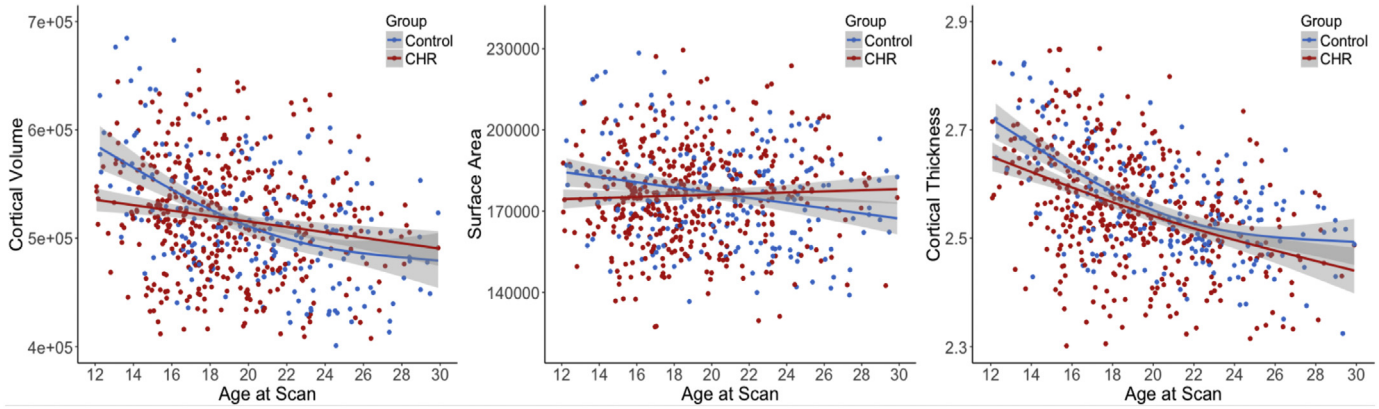

Fig. 3. GAM fitted age trajectories of total cortical gray matter volume, surface area, and mean thickness for individuals at CHR (n = 428) and healthy controls (n = 205). Shaded regions represent 95% confidence interval.

differences were tested across all surface area ROIs, individuals with poor premorbid functioning exhibited reductions in medial orbital frontal, lateral frontal, rostral anterior cingulate, precuneus, and temporal regions (See Table 6 for the complete list of ROIs). Smaller surface area was associated with poor functioning even when median childhood PAS score in the CHR group (PAS = 0.22) was used as a threshold (t = 4.19, P < .001), and also when the control subjects were excluded from the analysis (see supplementary materials). Neuroanatomical differences were not associated with PAS scores for the older group.

3.5. Antipsychotic medication exposure

Antipsychotic medication exposure at the time of baseline evaluation did not correlate with the cortical measures among either the younger CHR adolescents (cortical volume: F = 0.62, P = .43; surface area: F = 0.20, P = .28; cortical thickness: F = 2.29, P = .13; n = 121), or the older CHR adolescents (cortical volume: F = 0.12, P = .91; surface area: F = 0.09, P = .76; cortical thickness: F = 1.53, P = .21, n = 261).

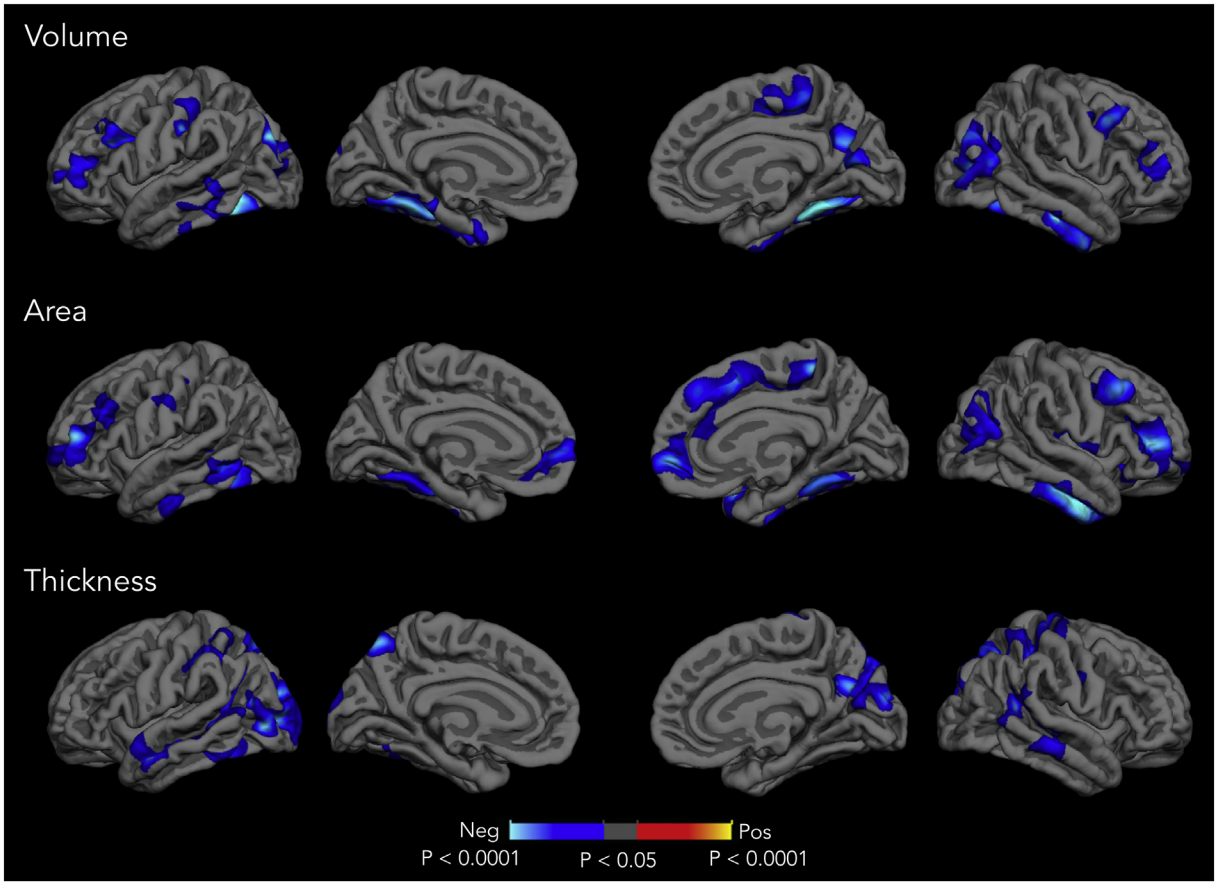

Fig. 4. Statistical P-value maps showing clusters in which individuals at CHR (n = 378) show significantly smaller cortical volume, surface area, and cortical thickness compared to healthy controls (n = 190). Regions exhibiting smaller cortical measures in CHR individuals than healthy controls are represented with a cooler color scheme. The effect was corrected for multiple comparisons by z Monte Carlo simulations and thresholded at P < .05. Uncorrected P values were displayed within the thresholded clusters.

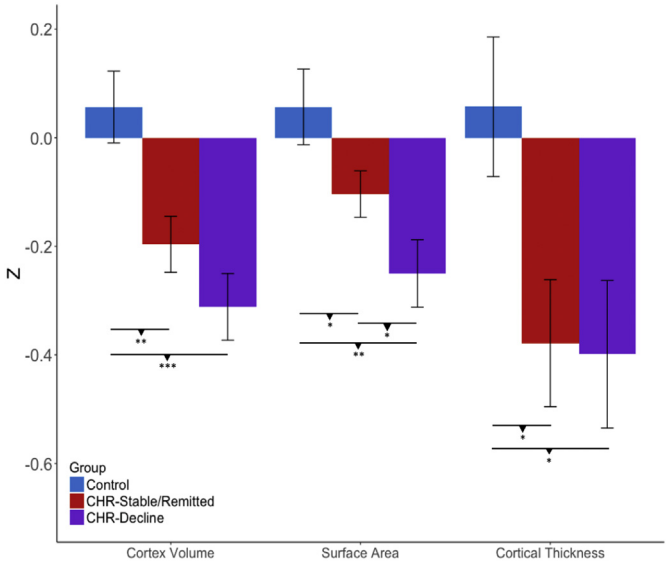

Fig. 5. Differences in cortex volume, surface area, and cortical thickness between CHR-Stable/Remitted (n = 87), CHR-Decline (n = 59), and healthy controls (n = 52) who are 17 years of age or under. P-values for post-hoc pairwise t-tests are indicated (uncorrected). *P < .05, **P < .01 *** P < .001.

4. Discussion

Widespread cortical deficiencies were predominantly observed among CHR individuals who were ascertained between 12 and 17 years of age compared to healthy controls at baseline evaluation. In contrast, group differences in the cortical measures were not observed among those who were 18 years of age or older. In terms of regional specificity for the younger group, vertex-wise between-group analysis revealed reduced cortical volume in dorsal lateral and medial prefrontal cortex, inferior parietal, parahippocampal, fusiform and inferior temporal regions, which resembles the spatial distribution of cortical deficits in multiple early disease stages of psychosis (Borgwardt et al., 2007; Fusar-Poli et al., 2011; Mechelli et al., 2011; Pantelis et al., 2003, 2005; Satterthwaite et al., 2016). Evidence of cortical volume loss in the CHR sample were further explained by a differential regional pattern of smaller cortical thickness and surface area. Given that cortical volume is a composite index reflecting both cortical thickness and surface area at each vertex, diminished cortical volume in dorsal lateral prefrontal, medio-orbital frontal, parahippocampal gyrus, and inferior parietal and temporal cortices were primarily driven by smaller surface area, while alterations in cortical thickness better explained cortical volume loss in pre- and post-central regions, precuneus, inferior temporal cortex, and lateral occipital cortex.

Aligned with our findings, youth with attenuated psychosis spectrum symptoms in the Philadelphia Neurodevelopmental Cohort (PNC) also showed reduced gray matter volume in similar brain regions including medial and orbital frontal cortex, dorsal lateral prefrontal cortex, precuneus, parahippocampal, and fusiform areas (Satterthwaite et al., 2016). Modest discrepancies in the results may be due to differences in the strategy of recruitment (community-based vs help-seeking), methodological differences in image processing, and demographic differences (age range). Nevertheless, given that both PNC and the NAPLS2 datasets have comparable sample size with an age range that encompasses early to mid-teenage years, the considerable overlap in regions showing cortical deficits in both cohort studies demonstrate manifestations of cortical abnormalities among individuals with attenuated symptoms of psychosis, especially among those who were ascertained in early adolescence.

We further investigated whether neuroanatomical deviance in early adolescence at the time of baseline evaluation is predictive of clinical outcome. While both better (CHR-Stable/Remitted) and poorer (CHR-Converted/Decline) clinical outcome group showed significant reduction in cortical indices compared to the healthy controls, regardless of their clinical outcome, the effect sizes of the poorer clinical outcome group were generally larger relative to the better outcome group. Within the CHR individuals, the group with poorer clinical outcomes showed significantly reduced surface area in superior, medial, and lateral prefrontal regions, rostral anterior cingulate, and parahippocampal gyrus compared with the better outcome group. This regional pattern is consistent with previous findings from at least two VBM studies, which have also reported gray matter volume loss in these brain regions among high-risk individuals who later developed psychosis compared with those who did not (Mechelli et al., 2011; Pantelis et al., 2003). Performing a surface-based analysis in the present study further revealed that the volumetric differences from previous studies might be driven by surface areal deficits and that this neuroanatomical profile might underlie insidious onset form of psychosis. Given that CHR individuals in both poorer and better outcome groups show cortical abnormalities, it does not appear that there is a critical threshold

Table 3
Between-group t-tests of CHR-Stable/Remitted (n = 87) versus healthy controls (n = 52) among subjects 17 years of age and under.

CHR-Stable/Remitted vs Healthy Control				
Hemisphere	ROI	Cohen's D	Uncorrected *P*-value	FDR Corrected *P*-value
Cortical thickness				
Right	Supramarginal	−0.52	0.005	0.094
	Postcentral	−0.48	0.005	0.094
	Posterior Cingulate	−0.44	0.017	0.13
	Superior Parietal	−0.41	0.017	0.15
	Inferior Parietal	−0.36	0.047	0.16
Left	Superior Temporal	−0.50	0.005	0.094
	Entorhinal	−0.52	0.005	0.094
	Supramarginal	−0.51	0.007	0.094
	Postcentral	−0.45	0.011	0.10
	Lateral Occiptal	−0.42	0.017	0.13
	Middle Temporal	−0.42	0.022	0.15
	Precuneus	−0.38	0.037	0.16
Surface area				
Right	Medial Orbital Frontal	−0.47	0.008	0.15
	Insula	−0.45	0.008	0.15
	Superior Temporal	−0.35	0.044	0.32
	Caudal Anterior Cingulate	−0.34	0.047	0.32
Left	Middle Temporal	−0.62	< 0.001	0.036
	Inferior Temporal	−0.50	0.006	0.15
	Caudal Anterior Cingulate	−0.41	0.016	0.21
	Medial Orbital Frontal	−0.35	0.04	0.32
Cortical volume				
Right	Medial Orbital Frontal	−0.54	0.0031	0.066
	Paracentral	−0.46	0.004	0.066
	Superior Temporal	−0.46	0.008	0.11
	Insula	−0.43	0.014	0.11
	Postcentral	−0.42	0.015	0.11
	Precuneus	−0.43	0.022	0.12
	Fusiform	−0.39	0.023	0.12
	Inferior Parietal	−0.37	0.031	0.14
Left	Middle Temporal	−0.61	0.0007	0.051
	Caudal Anterior Cingulate	−0.50	0.004	0.065
	Inferior Temporal	−0.48	0.012	0.11
	Postcentral	−0.44	0.012	0.11
	Entorhinal	−0.41	0.017	0.12
	Precuneus	−0.43	0.020	0.12
	Fusiform	−0.40	0.030	0.14
	Superior Temporal	−0.35	0.042	0.17

Table 4
Between group t-tests of CHR-Converted/Decline (n = 59) versus healthy controls (n = 52) among subjects 17 years of age and under.

CHR-Converted/Decline vs Healthy Control				
Hemisphere	ROI	Cohen's D	Uncorrected *P*-value	FDR Corrected *P*-value
Cortical thickness				
Right	Banks of Sup. Temporal Sulcus	−0.67	< 0.001	0.030
	Supramarginal	−0.65	0.001	0.030
	Caudal Middle Frontal	−0.54	0.006	0.081
	Inferior Parietal	−0.50	0.01	0.085
	Superior Parietal	−0.47	0.015	0.11
	Post Central	−0.46	0.015	0.11
	Cuneus	−0.44	0.021	0.12
	Superior Temporal	−0.42	0.029	0.15
	Pre Central	−0.37	0.047	0.19
Left	Superior Temporal	−0.65	0.001	0.030
	Middle Temporal	−0.57	0.004	0.071
	Inferior Temporal	−0.52	0.007	0.081
	Superior Parietal	−0.51	0.008	0.081
	Supra Marginal	−0.46	0.017	0.11
	Post Central	−0.49	0.037	0.18
	Superior Frontal	−0.40	0.040	0.18
	Lateral Occipital	−0.40	0.047	0.18
Surface area				
Right	Rostral Anterior Cingulate	−0.62	0.001	0.026
	Superior Frontal	−0.61	0.002	0.026
	Superior Temporal	−0.60	0.002	0.026
	Insula	−0.57	0.003	0.038
	Medial Orbito Frontal	−0.53	0.006	0.053
	Post Central	−0.49	0.011	0.069
	Fusiform	−0.48	0.014	0.085
	Caudal Anterior Cingulate	−0.45	0.019	0.088
	Middle Temporal	−0.44	0.021	0.088
	Rostral Middle Frontal	−0.42	0.026	0.10
	Paracentral	−0.41	0.029	0.11
	Inferior Temporal	−0.41	0.020	0.12
Left	Rostral Middle Frontal	−0.75	< 0.001	0.005
	Middle Temporal	−0.75	< 0.001	0.004
	Fusiform	−0.55	0.005	0.049
	Parahippocampal	−0.50	0.009	0.069
	Superior Frontal	−0.49	0.011	0.069
	Inferior Temporal	−0.46	0.019	0.089
	Banks of Superior Temporal Sulcus	−0.45	0.019	0.089
Cortical volume				
Right	Superior Temporal	−0.71	< 0.001	0.010
	Post Central	−0.68	< 0.001	0.010
	Banks of Superior Temporal Sulcus	−0.67	< 0.001	0.011
	Rostral Anterior Cingulate	−0.64	0.001	0.014
	Insula	−0.61	0.002	0.018
	Superior Frontal	−0.59	0.002	0.019
	Medial Orbito Frontal	−0.53	0.006	0.035
	Paracentral	−0.50	0.007	0.035
	Inferior Parietal	−0.51	0.007	0.035
	Caudal Anterior Cingulate	−0.48	0.013	0.054
	Middle Temporal	−0.48	0.013	0.054
	Cuneus	−0.45	0.018	0.067
	Fusiform	−0.43	0.026	0.091
	Precentral	−0.38	0.047	0.13
	Middle Temporal	−0.78	< 0.001	0.006
Left	Superior Temporal	−0.62	0.001	0.014
	Rostral Middle Frontal	−0.58	0.002	0.021
	Inferior Temporal	−0.56	0.005	0.030
	Banks of Superior Temporal Sulcus	−0.54	0.005	0.032
	Superior Frontal	−0.53	0.006	0.033
	Post Central	−0.47	0.019	0.061
	Fusiform	−0.42	0.029	0.094
	Paracentral	−0.38	0.048	0.12
	Rostral Anterior Cingulate	−0.39	0.048	0.12

Table 5
Between group t-tests of CHR-Stable/Remitted (n = 87) versus CHR-Converted/Decline (n = 59) among subjects 17 years of age and under.

CHR-Converted/Decline vs CHR-Stable/Remitted			
Hemisphere	ROI	Cohen's D	*P*-value
Right	Superior Frontal	−0.41	0.013
	Rosterior Anterior Cingulate	−0.34	0.034
Left	Rostral Middle Frontal	−0.41	0.014
	Parahippocampal	−0.42	0.015

that could reliability determine outcome in terms of a discrete construct, hence the preexisting neuroanatomical deviance as a marker of vulnerability for psychosis should be best regarded as a continuum.

Reduced surface area in superior and medial frontal cortex, precuneus, rostral anterior cingulate, and temporal regions among individuals in early adolescence were associated with poorer premorbid functioning in childhood. Interestingly, reduced surface area in many of these overlapping regions were also predictive of poorer clinical outcome. As the cerebral cortex undergoes rapid surface areal expansion and folding during the pre and peri-natal period, disturbances during early brain development could exert persisting effects on the dynamic cascade of post-natal brain maturation (Raznahan et al., 2012; Rees and Inder, 2005; Smith et al., 2015; Walhovd et al., 2012). Support for this view was observed in that normative variation of birth weight, which is a widely used proxy indicator of perinatal health, was robustly associated with surface area in widespread brain regions in typically developing individuals (Raznahan et al., 2012; Walhovd et al., 2012). In the context of schizophrenia, adult patients with history of obstetric complications such as intra-uterine growth retardation (IUGR) or fetal hypoxia manifested greater structural brain abnormalities (Cannon et al., 2002; van Erp et al., 2002). In particular, recent studies suggest that previously reported gray matter volumetric differences associated with obstetric complications among schizophrenia patients is better explained by smaller cortical surface area, rather than cortical thickness (Haukvik et al., 2009; Smith et al., 2015). Therefore, although we do not have prospective information of early life risk factors, such as objective records of obstetric history, for the NAPLS2 sample, it is plausible based on the prior literature that alterations in surface area among younger CHR adolescents may reflect manifestations of early neurodevelopmental insults. The mechanism behind the specificity of surface area deficits, which are predominantly observed in heteromodal association regions, is unclear; in the context of brain development, it could be that the developmental processes in phylogenically newer areas (higher-ordered association cortices) are more vulnerable to early life disturbances than the older regions (lower-order somatosensory and visual cortices) or it could be that neural insults specific to these regions

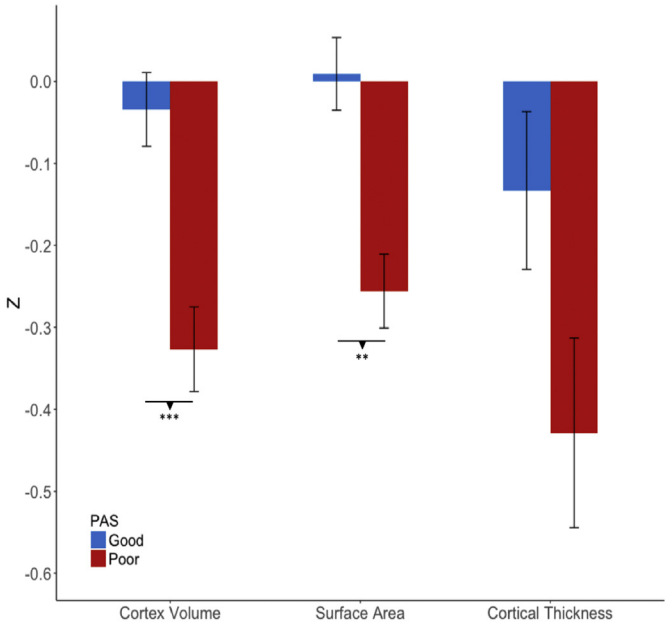

Fig. 6. Differences in cortex volume, surface area, and cortical thickness between individuals with poor (n = 87) versus good (n = 111) premorbid functioning among those who are 17 years of age or under (CHR and control individuals combined). *P*-values for post-hoc pairwise t-tests are indicated (uncorrected). $^{**}P < .01$ $^{***}P < .001$.

Table 6
Between group t-tests of PAS Good (n = 111) vs Poor (*n* = 87) among subjects 17 years of age and under.

PAS Good vs CHR-Poor				
Hemisphere	ROI	t	Uncorrected *P*-value	FDR Corrected *P*-value
Surface area				
Right	Medial Orbito Frontal	3.37	0.0009	0.015
	Banks of Sup. Temporal Sulcus	2.82	0.0008	0.045
	Rostral Anterior Cingulate	2.76	0.005	0.045
	Precuneus	2.74	0.006	0.045
Left	Precuneus	3.78	0.0002	0.014
	Inferior Temporal	3.58	0.0004	0.014
	Middle Temporal	3.38	0.0008	0.015
	Rostral Middle Frontal	3.19	0.0017	0.023
	Fusiform	2.96	0.0034	0.038
	Superior Frontal	2.86	0.0063	0.045

during early brain development become a risk factor for psychosis (as opposed to other kinds of neuropsychiatric outcomes).

Conversely, cortical thickness was not associated with premorbid functioning, suggesting that developmental factors that shape cortical thickness may be less sensitive to early life risk factors. Alterations in cortical thickness measures in younger CHR adolescents were generally observed in primary motor, sensory or in the posterior regions; parts of the brain that have been identified to mature earlier than higher order association areas in structural brain MRI measures (Gogtay et al., 2004; Tamnes et al., 2017). Non-linear monotonic decrease in cortical thickness that extends from childhood to early adulthood is thought to be a composite signal of numerous normal neuromaturational processes such as synaptic pruning, dendritic retraction and intracortical myelination (Catts et al., 2013; Huttenlocher, 1979; Huttenlocher and Dabholkar, 1997; Walhovd et al., 2016). In reflection of these normal brain maturational events, the rate of cortical thinning in the unimodal and the posterior regions reaches its peak in childhood, whereas cortical thinning in the associative and anterior regions typically extends through mid to late adolescence. Given that the spatiotemporal sequences of the cortical maturational pattern are highly regularized, reduced cortical thickness in the lower-order cortices in relation to psychosis risk may be a result of abnormal neuromaturational events or a disease process that co-occurs in the order in which these regions mature (i.e. starting with lower ordered posterior regions and continuing up to anterior associative regions). As another possibility, environmental risk factors, such as childhood trauma or drug abuse interacting with high genetic loading of schizophrenia, may have contributed to the alterations in cortical thickness (Habets et al., 2011). Nevertheless, further work is needed to replicate this pattern of findings and to clarify these interpretations.

In our previous work, brain age deviation score (i.e. brain age gap) did not correlate with premorbid functioning (Chung et al., 2018). This may be due to the fact that the version of the brain age model that we used considers different aspects of brain morphometry simultaneously (i.e., surface area, cortical thickness, subcortical volume) to predict chronological age, whereas premorbid functioning was specifically associated with surface area measures only, but not with cortical thickness. Given our interpretations that differential patterns of alterations in cortical thickness and surface area reflect heterogeneity in the etiology of neurodevelopmental disturbances, our findings suggest that the brain age metric is useful for quantifying gross deviation from normal developmental pattern of neuroanatomical changes at an individual subject level, but lacks sensitivity for detecting distinct patterns of neuroanatomical deviance that confers risk for psychosis.

Signs of neuroanatomical compromise were not observed among CHR individuals who were ascertained at 18 years of age or later. The null findings of cortical deficits between the groups could be explained by better sensitivity of CHR criteria in recruiting acute-onset forms of psychosis in late adolescence or early adulthood who are expected to be neuroanatomically similar to typically developing age-matched peers throughout most of the premorbid period but show a rapidly increasing deviation prior to the onset of psychosis (Cannon et al., 2015; Chung et al., 2018). Also, CHR individuals with more insidious onset who might show greater manifestations of pre-existing brain abnormalities are likely to be underrepresented among in the older group as they are more likely convert to psychosis before reaching late adolescence.

Our evaluation of the between-scanner reliabilities using the human traveling subject data indicate that raw ROI measures of surface area and subcortical volume were mostly in the good to superior range. In contrast, between-site reliabilities for cortical volume and cortical thickness measures were relatively modest. In this study, we adjusted for the scanner offsets based on prior knowledge in the literature that the shapes (or slopes) of growth curves of cortical measures in typically developing individuals are generalizable across independent datasets (Tamnes et al., 2017); this pattern was also observed in our dataset in which age regression slopes for each scanner were markedly parallel to each other. In this study, we showed that the scanner related adjustment we made improved between-site reliabilities of cortical thickness measures from mostly in the fair to good range into good to excellent range. A clear advantage of this approach is that the scanner related variance could be further reduced at *post-hoc* as long as there was sufficient sample size of healthy controls assessed at each scanner to reproduce the age related slope and intercept estimates.

There are some limitations to this study. Age at ascertainment is not an optimal measure for estimating age at prodromal symptom onset, as it does not consider the recency of when the symptoms emerged. This makes it difficult to model developmental trajectories of neuroanatomical structures as a function of age at onset. However, determining the age when prodromal symptoms first emerged is challenging as clinicians have to rely on subjects' retrospective memory to identify subtle symptoms that are linked to psychosis. Similarly, PAS also relies on retrospective memory; hence recalling the level of functioning during childhood is susceptible to bias, especially for the older participants as they have to recall more distant memories. Also, additional

investigation is required to confirm whether neuroanatomical abnormalities observed among the younger CHR cases are indeed linked to exposure to early neurodevelopmental risk factors (e.g., obstetric complications) as objective medical records of birth complications were not available for this sample. Prospective longitudinal birth cohort studies that are population-based or oversampled for psychosis risk with objective records (e.g., medical records, diary, video recordings, periodic psychological evaluation etc.) could address these limitations and further clarify the relationship between early life risk factors and developmental trajectories associated with onset of psychosis at different ages.

5. Conclusion

The novel contribution of this study is that deviance in neuroanatomical measures from normal developmental trajectories is predominantly observed in younger CHR individuals who present with an insidious onset pattern of psychosis. These early-manifesting cortical alterations overlap with brain regions that have previously been linked to schizophrenia and are associated with worsening clinical outcome in this sample. Based on this evidence, it would seem overly simplistic and highly misleading to view individuals experiencing attenuated symptoms of psychosis as a homogenous group with respect to variation in neuroanatomical structures (e.g., Fig. 3). Instead, variation in neuroanatomical measures must be considered with respect to the age of the individuals at the time of ascertainment for a psychosis risk syndrome, which in turn likely reflects heterogeneity in exposure to early risk factors and premorbid course. CHR individuals with poor premorbid functioning in childhood and earlier ages of prodromal symptom onset are expected to exhibit greater neuroanatomical deviation relative to age-matched peers prior to onset of psychosis. This interpretation suggests that structural brain measures assessed at baseline are likely to be sensitive primarily to “insidious” or “early” onset forms of psychosis among individuals at CHR. Nonetheless, this age moderated pattern needs to be replicated in independent datasets to confirm the generalizability of our findings. In addition, future work is encouraged to investigate whether the neuroanatomical profile linked to “early onset” forms of psychosis increase likelihood for experiencing later neuromaturational disturbances (e.g. disrupted synaptic pruning) once they become older adolescents.

Funding source

This work was supported by a collaborative U01 award from the National Institute of Mental Health at the National Institutes of Health (MH081902 to TDC; MH081857 to BAC; MH081988 to EW; MH076989-10 to DHM; MH081928 to LJS; MH082004 to DP; MH082022 to KC; MH081984 to JA; MH082022 to SWW) and NIMH P50 MH066286, NIH 1R01MH107250-02:S1, and Staglin Music Festival for Mental Health (CEB), NIMH P50 MH080272, and the Commonwealth of Massachusetts (SCDMH82101008006) to L.J.S.

Conflict of interests

The authors have declared that there are no conflicts of interest in relation to the subject of this study. Dr. Cannon and Dr. Mathalon reports that he is a consultant to Boerhinger Ingelheim Pharmaceuticals and Lundbeck A/S and is a co-inventor (with the other NAPLS investigators) on a pending patent of a blood-based predictive biomarker for psychosis. Dr. Perkins has served as a consultant for Sunovion and Alkemes and has received royalties from American Psychiatric Association Publishing.

Author contributions

Chung and Cannon had full access to all the data in the study and takes responsibility for the integrity of the data and the accuracy of the data analysis.

Acknowledgements

The research described in this paper was supported in part by a grant to Yoonho Chung from the American Psychological Association. The authors thank the following individuals for assistance with subject scheduling and/or scan acquisition: Angielette Andaya, Nurit Hirsh and Jamie Zinberg (UCLA); Richard Juelich (BIDMC-Harvard); M. Louis Lauzon, J. Stowkowy and C. Marshall (Calgary); Jason Nunag and Daniel Roman (UCSD); Nicole Popp Santamauro and Hedy Sarofin (Yale).

Appendix A. Supplementary data

Supplementary data to this article can be found online at https://doi.org/10.1016/j.nicl.2019.101862.

References

Addington, J.M., Cadenhead, K.S., Cornblatt, B.A., Mathalon, D.H., McGlashan, T.H., Perkins, D.O., et al., 2012. North American Prodrome longitudinal study (NAPLS 2): overview and recruitment. Schizophr. Res. 142 (1–3), 77–82. https://doi.org/10.1016/j.schres.2012.09.012.

Benjamini, Y., Hochberg, Y., 2000. On the adaptive control of the false discovery rate in multiple testing with independent statistics. J. Educ. Behav. Stat. 25 (1), 60–83. https://doi.org/10.3102/10769986025001060.

Borgwardt, S.J., Riecher-Rössler, A., Dazzan, P., Chitnis, X., Aston, J., Drewe, M., et al., 2007. Regional gray matter volume abnormalities in the at risk mental state. Bps 61 (10), 1148–1156. https://doi.org/10.1016/j.biopsych.2006.08.009.

Borgwardt, S.J., McGuire, P.K., Aston, J., Gschwandtner, U., Pflüger, M.O., Stieglitz, R.-D., et al., 2008. Reductions in frontal, temporal and parietal volume associated with the onset of psychosis. Schizophr. Res. 106 (2–3), 108–114. https://doi.org/10.1016/j.schres.2008.08.007.

Brown, T.T., Kuperman, J.M., Chung, Y., Erhart, M., McCabe, C., Hagler Jr., D.J., et al., 2012. Neuroanatomical assessment of biological maturity. Curr. Biol. 22 (18), 1693–1698. https://doi.org/10.1016/j.cub.2012.07.002.

Cannon, T.D., van Erp, T.G.M., Rosso, I.M., Huttunen, M., Lönnqvist, J., Pirkola, T., et al., 2002. Fetal hypoxia and structural brain abnormalities in schizophrenic patients, their siblings, and controls. Arch. Gen. Psychiatry 59 (1), 35–41.

Cannon, T.D., Sun, F., McEwen, S.J., Papademetris, X., He, G., van Erp, T.G.M., et al., 2013. Reliability of neuroanatomical measurements in a multisite longitudinal study of youth at risk for psychosis. Hum. Brain Mapp. 35 (5), 2424–2434. https://doi.org/10.1002/hbm.22338.

Cannon, T.D., Chung, Y., He, G., Sun, D., Jacobson, A., van Erp, T.G.M., et al., 2015. Progressive reduction in cortical thickness as psychosis develops: a multisite longitudinal neuroimaging study of youth at elevated clinical risk. Biol. Psychiatry 77 (2), 147–157. https://doi.org/10.1016/j.biopsych.2014.05.023.

Cannon-Spoor, H.E., Potkin, S.G., Wyatt, R.J., 1982. Measurement of premorbid adjustment in chronic schizophrenia. Schizophr. Bull. 8 (3), 470–484.

Catts, V.S., Fung, S.J., Long, L.E., Joshi, D., Vercammen, A., Allen, K.M., et al., 2013. Rethinking schizophrenia in the context of normal neurodevelopment. Front. Cell. Neurosci. 7, 60.

Chung, Y., Addington, J.M., Bearden, C.E., Cadenhead, K., Cornblatt, B., Mathalon, D.H., et al., 2018. Use of machine learning to determine deviance in neuroanatomical maturity associated with future psychosis in youths at clinically high risk. JAMA Psychiatry 1–9. https://doi.org/10.1001/jamapsychiatry.2018.1543.

Cicchetti, D.V., Sparrow, S.A., 1981. Developing criteria for establishing interrater reliability of specific items: applications to assessment of adaptive behavior. Am. J. Ment. Defic. 86 (2), 127–137.

Dale, A.M., Fischl, B., Sereno, M.I., 1999. Cortical surface-based analysis. I. Segmentation and surface reconstruction. NeuroImage 9 (2), 179–194. https://doi.org/10.1006/nimg.1998.0395.

Desikan, R.S., Ségonne, F., Fischl, B., Quinn, B.T., Dickerson, B.C., Blacker, D., et al., 2006. An automated labeling system for subdividing the human cerebral cortex on MRI scans into gyral based regions of interest. NeuroImage 31 (3), 968–980. https://doi.org/10.1016/j.neuroimage.2006.01.021.

Dewey, J., Hana, G., Russell, T., Price, J., McCaffrey, D., Harezlak, J., et al., 2010. Reliability and validity of MRI-based automated volumetry software relative to auto-assisted manual measurement of subcortical structures in HIV-infected patients from a multisite study. NeuroImage 51 (4), 1334–1344. https://doi.org/10.1016/j.neuroimage.2010.03.033.

First, M.B., Spitzer, R.L., Gibbon, M., Williams, J.B., 1995. Structured Clinical Interview for DSM-IV Axis I Disorders. Patient Edition. Research Department, New York State Psychiatric Institute, New York.

Fischl, B., 2004. Automatically parcellating the human cerebral cortex. Cereb. Cortex 14 (1), 11–22. https://doi.org/10.1093/cercor/bhg087.

Fischl, B., Dale, A.M., 2000. Measuring the thickness of the human cerebral cortex from

magnetic resonance images. Proc. Natl. Acad. Sci. U. S. A. 97 (20), 11050–11055. https://doi.org/10.1073/pnas.200033797.
Fischl, B., Sereno, M.I., Dale, A.M., 1999. Cortical surface-based analysis: II: inflation, flattening, and a surface-based coordinate system. NeuroImage 9 (2), 195–207.
Fischl, B., Salat, D.H., Busa, E., Albert, M., Dieterich, M., Haselgrove, C., et al., 2002. Whole brain segmentation: automated labeling of neuroanatomical structures in the human brain. Neuron 33 (3), 341–355.
Fjell, A.M., Walhovd, K.B., Westlye, L.T., Østby, Y., Tamnes, C.K., Jernigan, T.L., et al., 2010. When does brain aging accelerate? Dangers of quadratic fits in cross-sectional studies. NeuroImage 50 (4), 1376–1383. https://doi.org/10.1016/j.neuroimage.2010.01.061.
Friedman, L., Stern, H., Brown, G.G., Mathalon, D.H., Turner, J., Glover, G.H., et al., 2007. Test-retest and between-site reliability in a multicenter fMRI study. Hum. Brain Mapp. 29 (8), 958–972. https://doi.org/10.1002/hbm.20440.
Fusar-Poli, P., Borgwardt, S., Crescini, A., Deste, G., Kempton, M.J., Lawrie, S., et al., 2011. Neuroanatomy of vulnerability to psychosis: a voxel-based meta-analysis. Neurosci. Biobehav. Rev. 35 (5), 1175–1185. https://doi.org/10.1016/j.neubiorev.2010.12.005.
Fusar-Poli, P., Bonoldi, I., Yung, A.R., Borgwardt, S., Kempton, M.J., Valmaggia, L., et al., 2012. Predicting psychosis: meta-analysis of transition outcomes in individuals at high clinical risk. Arch. Gen. Psychiatry 69 (3), 220–229.
Gogtay, N., Giedd, J.N., Lusk, L., Hayashi, K.M., Greenstein, D., VaituzisAITUZIS, A.C., et al., 2004. Dynamic mapping of human cortical development during childhood through early adulthood. Proc. Natl. Acad. Sci. U. S. A. 101 (21), 8174–8179. https://doi.org/10.1073/pnas.0402680101.
Habets, P., Marcelis, M., Gronenschild, E., Drukker, M., van Os, J., Genetic Risk and Outcome of Psychosis (G.R.O.U.P), 2011. Reduced cortical thickness as an outcome of differential sensitivity to environmental risks in schizophrenia. Biol. Psychiatry 69 (5), 487–494. https://doi.org/10.1016/j.biopsych.2010.08.010.
Hagler Jr., D.J., Saygin, A.P., Sereno, M.I., 2006. Smoothing and cluster thresholding for cortical surface-based group analysis of fMRI data. NeuroImage 33 (4), 1093–1103. https://doi.org/10.1016/j.neuroimage.2006.07.036.
Haukvik, U.K., Lawyer, G., Bjerkan, P.S., Hartberg, C.B., Jönsson, E.G., McNeil, T., Agartz, I., 2009. Cerebral cortical thickness and a history of obstetric complications in schizophrenia. J. Psychiatr. Res. 43 (16), 1287–1293. https://doi.org/10.1016/j.jpsychires.2009.05.001.
Hayasaka, S., 2003. Validating cluster size inference: random field and permutation methods. NeuroImage 20 (4), 2343–2356. https://doi.org/10.1016/j.neuroimage.2003.08.003.
Huttenlocher, P.R., 1979. Synaptic density in human frontal cortex—developmental changes and effects of aging. Brain Res. 163 (2), 195–205. https://doi.org/10.1016/0006-8993(79)90349-4.
Huttenlocher, P.R., Dabholkar, A.S., 1997. Regional differences in synaptogenesis in human cerebral cortex. J. Comp. Neurol. 387 (2), 167–178.
Jernigan, T.L., Brown, T.T., Hagler Jr., D.J., Akshoomoff, N., Bartsch, H., Newman, E., et al., 2016. The pediatric imaging, Neurocognition, and genetics (PING) data repository. NeuroImage 124, 1149–1154. https://doi.org/10.1016/j.neuroimage.2015.04.057.
Koutsouleris, N., Meisenzahl, E.M., Davatzikos, C., Bottlender, R., Frodl, T., Scheuerecker, J., et al., 2009. Use of neuroanatomical pattern classification to identify subjects in at-risk mental states of psychosis and predict disease transition. Arch. Gen. Psychiatry 66 (7), 700–712.
Lyngberg, K., Buchy, L., Liu, L., Perkins, D., Woods, S., Addington, J.M., 2015. Patterns of premorbid functioning in individuals at clinical high risk of psychosis. Schizophr. Res. 169 (1–3), 209–213. https://doi.org/10.1016/j.schres.2015.11.004.
McGlashan, T., Walsh, B., Woods, S., 2010. The Psychosis-Risk Syndrome: Handbook for Diagnosis and Follow-Up. Oxford University Press.
Mechelli, A., Riecher-Rössler, A., Meisenzahl, E.M., Tognin, S., Wood, S.J., Borgwardt, S.J., et al., 2011. Neuroanatomical abnormalities that predate the onset of psychosis: a multicenter study. Arch. Gen. Psychiatry 68 (5), 489–495. https://doi.org/10.1001/archgenpsychiatry.2011.42.
Miller, T.J., McGlashan, T.H., Rosen, J.L., Somjee, L., Markovich, P.J., Stein, K., Woods, S.W., 2002. Prospective diagnosis of the initial prodrome for schizophrenia based on the structured interview for prodromal syndromes: preliminary evidence of interrater reliability and predictive validity. Am. J. Psychiatr. 159 (5), 863–865.
Mueller, S.G., Weiner, M.W., Thal, L.J., Petersen, R.C., Jack, C.R., Jagust, W., et al., 2005. Ways toward an early diagnosis in Alzheimer's disease: the Alzheimer's disease neuroimaging initiative (ADNI). Alzheimer. Dementia 1 (1), 55–66. https://doi.org/10.1016/j.jalz.2005.06.003.
Nugent, A.C., Luckenbaugh, D.A., Wood, S.E., Bogers, W., Zarate, C.A., Drevets, W.C., 2013. Automated subcortical segmentation using FIRST: test-retest reliability, inter-scanner reliability, and comparison to manual segmentation. Hum. Brain Mapp. 34 (9), 2313–2329. https://doi.org/10.1002/hbm.22068.
Pantelis, C., Velakoulis, D., McGorry, P.D., Wood, S.J., Suckling, J., Phillips, L.J., et al., 2003. Neuroanatomical abnormalities before and after onset of psychosis: a cross-sectional and longitudinal MRI comparison. Lancet 361 (9354), 281–288.
Pantelis, C., Yücel, M., Wood, S.J., Velakoulis, D., Sun, D., Berger, G., et al., 2005. Structural brain imaging evidence for multiple pathological processes at different stages of brain development in schizophrenia. Schizophr. Bull. 31 (3), 672–696. https://doi.org/10.1093/schbul/sbi034.
Raznahan, A., Greenstein, D., Lee, N.R., Clasen, L.S., Giedd, J.N., 2012. Prenatal growth in humans and postnatal brain maturation into late adolescence. Proc. Natl. Acad. Sci. 109 (28), 11366–11371. https://doi.org/10.1073/pnas.1203350109.
Rees, S., Inder, T., 2005. Fetal and neonatal origins of altered brain development. Early Hum. Dev. 81 (9), 753–761. https://doi.org/10.1016/j.earlhumdev.2005.07.004.
Satterthwaite, T.D., Wolf, D.H., Calkins, M.E., Vandekar, S.N., Erus, G., Ruparel, K., et al., 2016. Structural brain abnormalities in youth with psychosis spectrum symptoms. JAMA Psychiatry 73 (5), 510–515. https://doi.org/10.1001/jamapsychiatry.2015.3463.
Schnack, H.G., van Haren, N.E.M., Brouwer, R.M., van Baal, G.C.M., Picchioni, M., Weisbrod, M., et al., 2010. Mapping reliability in multicenter MRI: voxel-based morphometry and cortical thickness. Hum. Brain Mapp. 31 (12), 1967–1982. https://doi.org/10.1002/hbm.20991.
Smith, G.N., Thornton, A.E., Lang, D.J., MacEwan, G.W., Kopala, L.C., Su, W., Honer, W.G., 2015. Cortical morphology and early adverse birth events in men with first-episode psychosis. Psychol. Med. 45 (9), 1825–1837. https://doi.org/10.1017/S003329171400292X.
Sun, D., Phillips, L., Velakoulis, D., Yung, A., McGorry, P.D., Wood, S.J., et al., 2009. Progressive brain structural changes mapped as psychosis develops in “at risk” individuals. Schizophr. Res. 108 (1–3), 85–92. https://doi.org/10.1016/j.schres.2008.11.026.
Takahashi, T., Wood, S.J., Yung, A.R., Phillips, L.J., Soulsby, B., McGorry, P.D., et al., 2009. Insular cortex gray matter changes in individuals at ultra-high-risk of developing psychosis. Schizophr. Res. 111 (1–3), 94–102. https://doi.org/10.1016/j.schres.2009.03.024.
Tamnes, C.K., Herting, M.M., Goddings, A.-L., Meuwese, R., Blakemore, S.-J., Dahl, R.E., Güroğlu, B., Raznahan, A., Sowell, E.R., Crone, E.A., Mills, K.L., 2017. Development of the cerebral cortex across adolescence: a multisample study of inter-related longitudinal changes in cortical volume, surface area, and thickness. J. Neurosci. 37 (12), 3402–3412. https://doi.org/10.1523/JNEUROSCI.3302-16.2017.
van Erp, T.G.M., Saleh, P.A., Rosso, I.M., Huttunen, M., Lönnqvist, J., Pirkola, T., et al., 2002. Contributions of genetic risk and fetal hypoxia to hippocampal volume in patients with schizophrenia or schizoaffective disorder, their unaffected siblings, and healthy unrelated volunteers. Am. J. Psychiatr. 159 (9), 1514–1520. https://doi.org/10.1176/appi.ajp.159.9.1514.
Van Mastrigt, S., Addington, J.M., 2002. Assessment of premorbid function in first-episode schizophrenia: modifications to the premorbid adjustment scale. J. Psychiatry Neurosci. 27 (2), 92–101.
Velakoulis, D., Wood, S.J., Wong, M.T.H., McGorry, P.D., Yung, A., Phillips, L., et al., 2006. Hippocampal and amygdala volumes according to psychosis stage and diagnosis: a magnetic resonance imaging study of chronic schizophrenia, first-episode psychosis, and ultra-high-risk individuals. Arch. Gen. Psychiatry 63 (2), 139–149. https://doi.org/10.1001/archpsyc.63.2.139.
Walhovd, K.B., Fjell, A.M., Brown, T.T., Kuperman, J.M., Chung, Y., Hagler, D.J., et al., 2012. Long-term influence of normal variation in neonatal characteristics on human brain development. Proc. Natl. Acad. Sci. U. S. A. 109 (49), 20089–20094. https://doi.org/10.1073/pnas.1208180109/-/DCSupplemental.
Walhovd, K.B., Fjell, A.M., Giedd, J., Dale, A.M., Brown, T.T., 2016. Through thick and thin: a need to reconcile contradictory results on trajectories in human cortical development. Cereb. Cortex, bhv301. https://doi.org/10.1093/cercor/bhv301.
Woods, S.W., Walsh, B.C., Addington, J.M., Cadenhead, K.S., Cannon, T.D., Cornblatt, B.A., et al., 2014. Current status specifiers for patients at clinical high risk for psychosis. Schizophr. Res. 158 (1–3), 69–75. https://doi.org/10.1016/j.schres.2014.06.022.